ELSEVIER

Ceramics International 27 (2001) 1–7

CERAMICS INTERNATIONAL

www.elsevier.com/locate/ceramint

Porous mullite ceramics from national clay produced by gelcasting

Ya-Fei Liu, Xing-Qin Liu, Hui Wei, Guang-Yao Meng *

Department of Materials Science and Engineering, University of Science and Technology of China, Anhui 230026, PR China

Received 19 January 2000; received in revised form 14 February 2000; accepted 24 March 2000

Abstract

Gelcasting process has been successfully employed to fabricate porous mullite ceramics in this work. The specimens based on mullite composition are found with open porosity of 58.5–63.9%, mean pore size of 0.76–1.31 μm, and nitrogen permeability of 526–1240 $m^3\ m^{-2}\ bar^{-1}\ h^{-1}$ by reactively sintering the gelled mixture of kaolinite and aluminum hydroxide at 1300–1600°C. The porosity, mean pore size, pore size distribution and gas permeability can be controlled by adjusting raw material ratios and sintering temperatures. The gas permeability of the specimens is found to be more dependent on the average pore size than on the open porosity. In addition, the gas transportation mechanism in porous mullite ceramics is dominated by laminar flow when the specimens are fired at high temperatures.

Keywords: B. Porosity; C. Diffusion; D. Mullite; Gelcasting

1. Introduction

In the last few years, porous ceramics found increasing attention for their successful applications in bioceramics [1], catalyst supports [2], hot gases filter [3], liquid food production [4], sensors [5], and membrane reactors [6]. As a porous support material, mullite was reported because of its good thermal shock resistance, strength and stability properties [7]. The applications of pure mullite made by wet chemical methods (e.g. sol–gel, hydrolysis, coprecipitation, ultrasonic spray pyrolysis, polymer decomposition, hydrothermal synthesis and chemical vapor deposition) are limited for their expensive production cost. The cost, however, will be reduced largely if national clays are used as starting materials.

Porous mullite ceramics based on national clay such as kaolinite and allophane were reported by others [8–12]. In general, there is a high volume fraction of glassy phase due to existence of amorphous silica or impurities in the calcined clays. Therefore, the pores were usually produced by leaching out the coexisting silica glass phase from fired clays with the solutions of caustic soda [8,10], caustic potash [9], acid [11], or a combined employment of caustic soda and hydrochloric acid [12]. In order to get rapid and complete leaching, some processes were completed even on the hydrothermal and microwave conditions [10]. The open porosity and the average pore size reported in literatures were 40–57% and 0.17–0.61 μm, respectively. These pore sizes are not large enough to provide for gas or water permeability if porous mullite ceramics are for the filter purpose.

Gelcasting is a new shaping process based on the theory of the in-situ polymerization of monomers in a ceramic slurry, which forms a strong and cross-linked polymer-solvent gel after poured into a mold. This process aimed at forming complex-shaped and near-net-shaped advanced ceramic materials originally [13], and later was applied to produce textured ceramic laminates [14], porous ceramics [15], ceramic powders [16] and nano-sized ceramics [17]. Recently, an automated gelcasting fabrication process was developed to manufacture large-scale ceramic turbine rotors, and the production was said to be at least 500 rotors per month [18]. Therefore, gelcasting will surely become an important method to produce various-shaped ceramic parts.

In this work, we try to develop this process to prepare porous mullite ceramics. An investigation on the relationship among phase compositions, microstructure, pore properties and preparation conditions is presented.

* Corresponding author. Tel.: +86-551-360-3234; fax: +86-551-363-1760.

E-mail address: mgym@ustc.edu.cn (G.-Y. Meng).

0272-8842/01/$20.00
PII: S0272-8842(00)00034-1

2. Experimental procedure

2.1. Specimen preparation

High-purity kaolinite (China Kaolinite Company) and aluminum hydroxide (Shandong Aluminum Industry Company) were used as the raw materials. The particle size distributions of raw materials powders used in this study were analyzed by a laser analyzer (Coulter LS100, USA), and the mean diameters of kaolinite and aluminum hydroxide are 12.06 and 6.14 μm, respectively. The mixtures of kaolinite and aluminum hydroxide with different ratios were fired previously at 600°C for 2 h, then mixed in an aqueous solution of monomers (acrylamide, AM and *N,N′*-methylene-bis-acrylamide, MBAM), whose total amount is about 5 wt.% of the ceramic powders, and ball-milled for more than 10 h. Some dispersants were added to get a well-dispersed slurry. After initiated by ammonium bisulphate and catalyzed by TEMED, the resulting slurry was molded in a vibrating table, then became gelled within a few minutes. The gelled ceramics were demolded, dried, machined, and then sintered in a programmable HT furnace (Nabertherm, Germany) under different temperature from 1300 to 1600°C for 5 h.

2.2. Characterizations of the specimens

The differential thermal analysis and thermogravimetry (DTA–TG) of the dried green gelcasts were examined by a thermal analyzer from 40 to 1070°C at a heating rate of 10°C min^{-1}. The compositions of the fired specimens were identified by XRD (Kigaku D/MAz-γ_A rotating X-ray diffraction unit) and their microstructures were observed by means of SEM (Hitachi X-650 scanning electronic microscope, Japan). The density, open porosity, and total porosity were determined by Archmede's method with the theoretical density of 3.23 g cm^{-3} for mullite. The average pore size and pore size distribution of the sintered porous specimens were obtained by the bubble-point method and pure nitrogen flux through the porous disks was measured in a permeation device.

3. Results and discussion

3.1. DTA–TG analysis of the green body

DTA–TG was used in analyzing the thermal decomposition and the phase transformation during heating the dried green body with 71.8 wt.% Al_2O_3 in the air, and the results are shown in Fig. 1. At $T<130$°C, there are a small endothermal DTA peak and about 5% mass loss, which are caused by the removal of occluded water in the gelcast specimens. In the temperature range of 300–400°C, there is a small exothermal DTA peak accompanied by another 5% mass loss, which is ascribed to the burn-out of the cross-linked polymer network. Because the ceramic powders were pre-heated at 600°C, during which kaolinite transformed into metakaolinite and aluminum hydroxide into alumina, no weight loss or thermal effect is shown for the phase changes in ceramics themselves below 600°C. Between 840 and 1000°C, a large exothermal DTA peak appears, which is attributed to the phase transformation from metakaolinite to Al–Si spinel [19].

3.2. X-ray diffraction investigations

The gelcasts with different Al_2O_3 wt.% were sintered at 1500°C for 5 h, and the products were identified by XRD in Fig. 2. The specimen made of mere kaolinite shows complete orthorhombic mullite diffraction peaks in addition to the heavy background, the later is due to the existence of non-crystalline silica glassy phases which formed from the decomposition of kaolinite (Fig. 2d). On the other hand, the sample based on only aluminum hydroxide turns out to be corundum entirely at 1500°C (Fig. 2a). For the specimens of their mixtures ($Al_2O_3=60\sim71.8$ wt.%), however, not only mullite but also a little corundum formed in the products. And the corundum amount rises as Al_2O_3 wt.% increases (Fig. 2b and c).

The green bodies with 71.8 wt.% Al_2O_3 were fired at 1400, 1500 and 1600°C for 5 h separately, and their XRD patterns are shown in Fig. 3. In order to understand the reaction mechanism, the gelcast based on the kaolinite alone was also fired at 1400°C for 5 h (Fig. 3a). The results prove that the final phase compositions depend greatly on the treating temperatures. Mullite increases steadily in its amount, while corundum decreases and nearly disappears at last from 1400 to 1600°C. At 1400°C, the specimen of mere kaolinite shows a big peak around $d=0.411$ nm ($2\theta=21.6$°), which stands for the typical major diffraction of (111) face of cristobalite. However, there isn't this peak in the

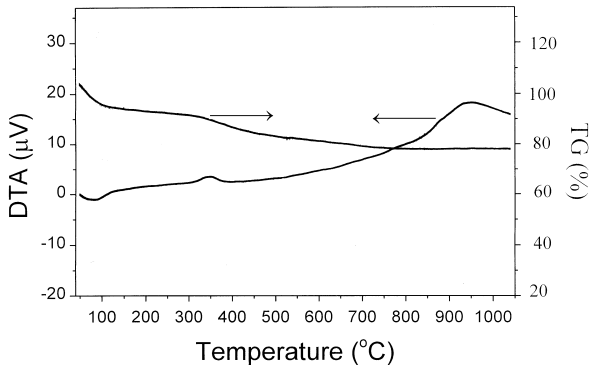

Fig. 1. DTA–TA curves of the green gelcast with 71.8 wt.% Al_2O_3.

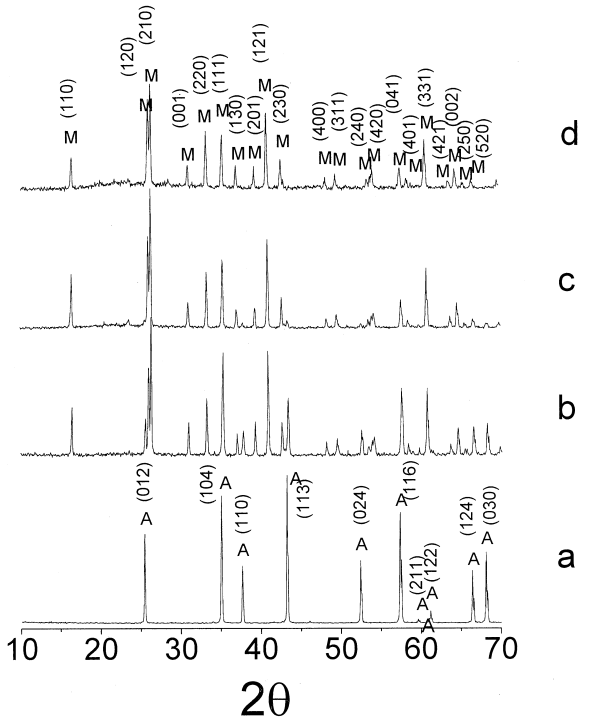

Fig. 2. XRD patterns of the specimens with different raw material ratios fired at 1500°C/5 h: (a) aluminum hydroxide; (b) 71.8 wt.% Al_2O_3 ceramics; (c) 60 wt.% Al_2O_3 ceramics; (d) kaolinite (M, mullite, A, corundum).

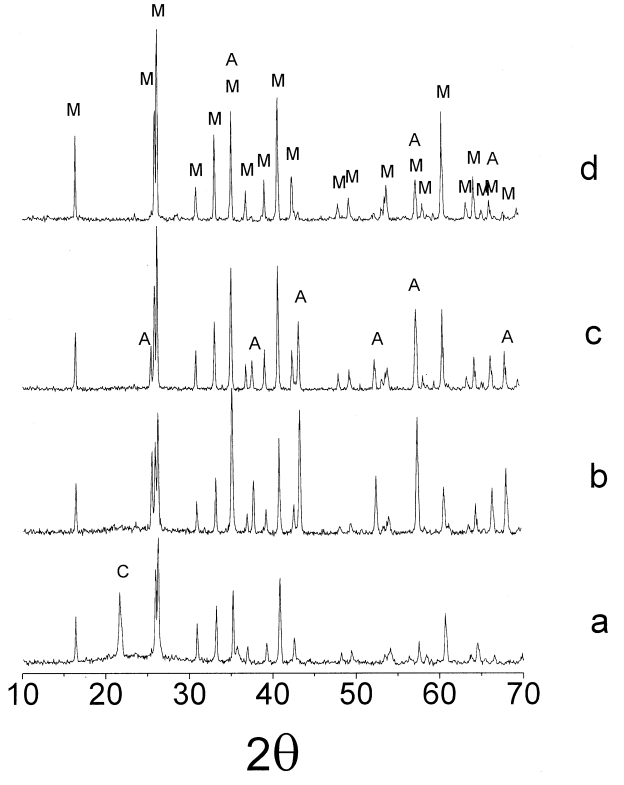

Fig. 3. XRD patterns of the specimens fired at different temperatures: (a) kaolinite, 1400°C/5 h; (b) 71.8 wt.% Al_2O_3 ceramics, 1400°C/5 h; (c) 71.8 wt.% Al_2O_3 ceramics, 1500°C/5 h; (d) 71.8 wt.% Al_2O_3 ceramics, 1600°C/5 h (M, mullite, A, corundum, C, cristobalite).

case of the 71.8 wt.% Al_2O_3 ceramics heated at the same conditions. It means that in addition to the primary mullite, which was produced solely from kaolinite, the secondary mullite formed from the reaction between silica and alumina when the specimens were fired at enough high temperature.

3.3. Pore parameters of sintered specimens

3.3.1. Open porosity, closed porosity and total porosity

The effects of the preparation conditions (e.g. the raw material ratios, the sintering temperatures) on the open porosity of the fired specimens were illustrated in Fig. 4. For the ceramic samples made by firing kaolinite (~43.7 wt.% Al_2O_3) or aluminum hydroxide (100 wt.% Al_2O_3) alone, the open porosity (ρ_o) depends more closely on the sintering temperature than that made of their mixtures. The specimen made of mere kaolinite is found having the largest sintering shrinkage due to the formation of large amount of glassy phase and thus is the densest sample with the lowest porosity ($\rho_o = 8.6$–35.8%) at any heating temperatures. In all cases, ρ_o keeps on increasing with Al_2O_3% when the later is not more than 75%. Compared with 75%Al_2O_3 ceramics ($\rho_o = 60.5$–64.2%), the specimen based on aluminum hydroxide alone has slightly higher porosity at 1300–1400°C (66.2–67.4%), and smaller porosity at 1500–1600°C (51.1–54.6%). This means corundum began to sinter only when fired at a temperature higher than 1400°C. It can also be learned from Fig. 4 that all specimens become increasingly dense as the heating temperature rises, and the open porosity of the ceramics near the theoretical mullite constituent is less dependent on the treating temperatures. As for case of the mullite

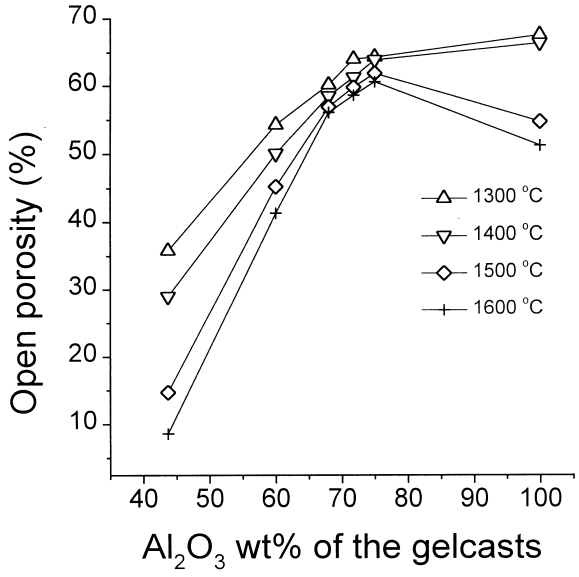

Fig. 4. Open porosity of the specimens with different Al_2O_3% fired at different temperatures.

ceramics (~71.8% Al_2O_3) shown in Fig. 5, its open porosity decreases from 63.9 to 58.5% with the increasing temperature, while the closed porosity is very small and nearly constant (~0.7%). Both Figs. 4 and 5 imply that the open porosity should be able to be controlled by adjusting the raw material ratio and the heating temperature.

3.3.2. Pore size distributions and average pore sizes

The raw material ratios also have influence on the mean pore sizes and pore size distributions of the ceramics fired at 1500°C for 5 h, as shown in Fig. 6. As

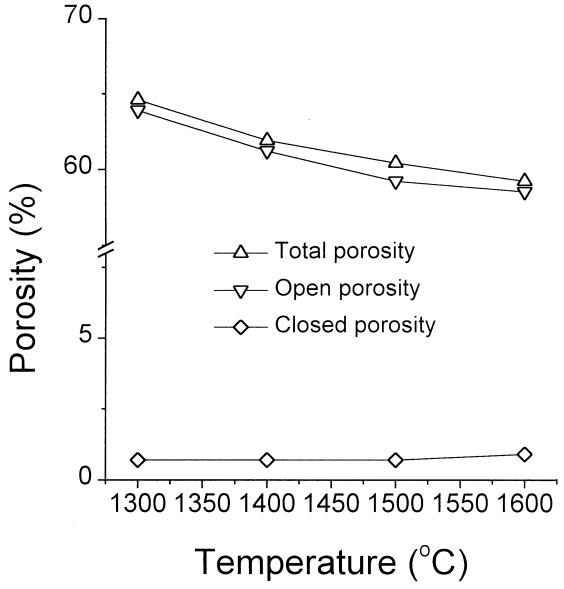

Fig. 5. Effect of the sintering temperature on the porosity of the fired 71.8 wt.% Al_2O_3 ceramics.

Al_2O_3% rises, both the mean pore diameter and maximum pore diameter increase gradually, and the mean pore diameters of the specimens with 60, 65, 68, 71.8, 75 and 100% Al_2O_3 are 0.91, 1.11, 1.13, 1.17, 1.19 and 1.21 μm, respectively. The small pore sizes of the specimens with low Al_2O_3% are ascribable to the existence of glassy silica phase, which formed from the decomposition of metakaolinite at around 1000°C and diffused into the small openings produced by burn-out of the cross-linked polymer network at 300–400°C (c.f. Fig. 1). High Al_2O_3% specimens, however, provide more alumina to react with the glassy silica and thus raises the pore size.

The pore size distributions of the mullite ceramics (~71.8 wt.% Al_2O_3) are closely related to the sintering temperatures (Fig. 7). The average pore size rises with the sintering temperature, and the values are 0.76, 0.90, 1.17 and 1.31 μm for 1300, 1400, 1500 and 1600°C, respectively. When sintered at higher temperature, more big pores larger than 1.5 μm appeared in the materials according to Fig. 7. In general, the average pore size will be minified when a porous ceramics is sintered with increasing temperature. The phenomenon here is abnormal and the similar case was ever found in the porous YSZ ceramics by gelcasting [15]. This is partly because the growth of mullite leaded to the formation of large pores and elimination of smaller pores, partly because the glassy silica existing in the specimens reacted with corundum and released big pores at increasing temperature.

3.3.3. Gas permeability

Fluid permeability or fluid flux is an important parameter for a porous ceramics. Fig. 8 illustrates the nitrogen fluxes of the specimens with different Al_2O_3%

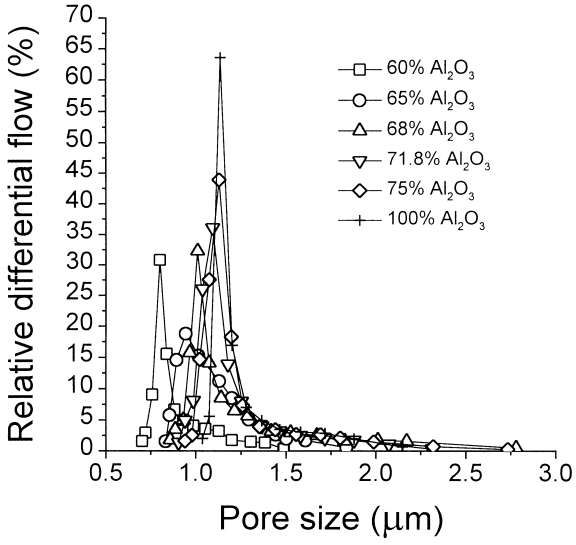

Fig. 6. Pore size distributions of the specimens with different raw material ratios fired at 1500°C for 5 h.

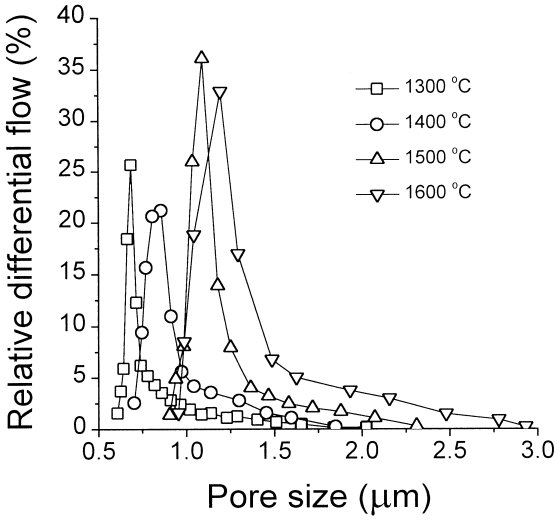

Fig. 7. Pore size distributions of the 71.8 wt.% Al_2O_3 specimens fired at different temperatures.

fired at 1500°C for 5 h. The gas flux increases with the pressure drop as well as Al_2O_3%, and its values are 537, 690, 849 and 1048 $m^3\ m^{-2}\ bar^{-1}\ h^{-1}$, respectively for 60, 65, 71.8 and 100% Al_2O_3 ceramics. The flux change trend for most ceramic specimens agrees well with that of mean pore size (Fig. 6) and open porosity (Fig. 4). An exception is for the gelcast based on sole aluminum hydroxide, whose gas flux is the largest though its open porosity is a little smaller than that of 75% Al_2O_3 ceramics. It suggests that the gas flux is more dependent on the mean pore size than on the open porosity.

The nitrogen fluxes of the same specimens as presented in Fig. 7 are illustrated in Fig. 9. The flux goes up with the pressure drop and sintering temperature, its values are 526, 720, 849, and 1243 $m^3\ m^{-2}\ bar^{-1}\ h^{-1}$ for

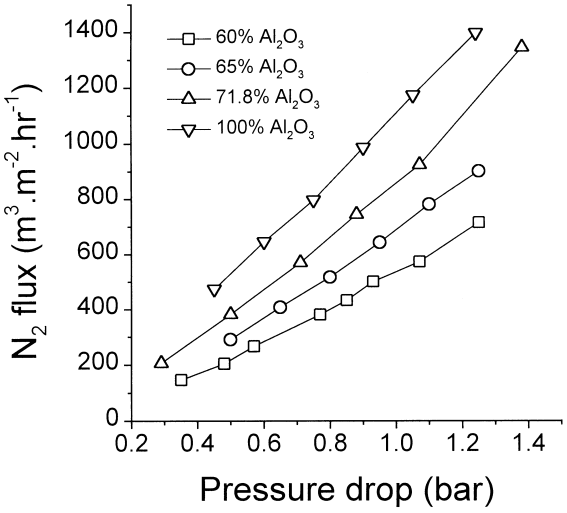

Fig. 8. Nitrogen fluxes of the specimens with different raw material ratios fired at 1500°C for 5 h.

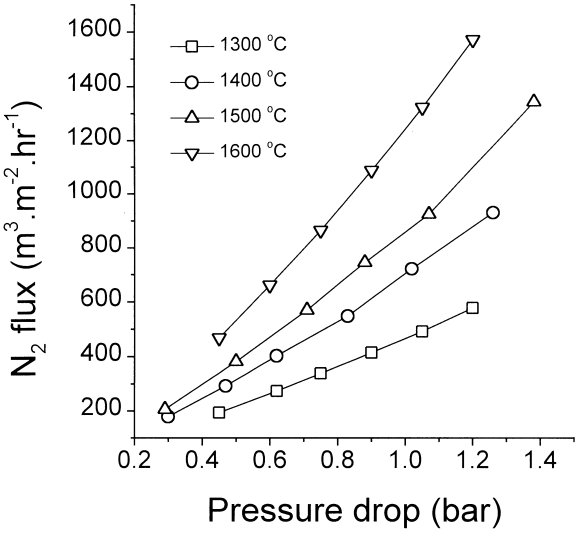

Fig. 9. Nitrogen fluxes of the 71.8 wt.% Al_2O_3 specimens fired at different temperatures for 5 h.

1300, 1400, 1500 and 1600°C, respectively. The flux change trend is in agreement with that of mean pore sizes in Fig. 7 but against that of open porosity in Fig. 5. Though the open porosity drops when fired at increasing temperature, its value changes a little. Thus, it brings little influence on the gas flux other than mean pore size.

3.4. Mechanism of gas permeability

When a gas flows in a porous material, its permeability can be represented by the following equation [20],

$$F_o = \frac{F}{A\Delta P} = C_1 + C_2 P_m \quad (1)$$

where F_o is the permeability (mol $m^{-2}\ s^{-1}\ Pa^{-1}$), F the flow (mol s^{-1}), A the outer surface area (m^2), ΔP the pressure drop, P_m the average pressure in the porous material, C_1 and C_2 two constants representing Knudsen diffusion and laminar flow, respectively.

According to Eq. (1), the plots of permeability in the mullite ceramics versus mean pressure are illustrated in Fig. 10. It is found that good linear relationships exist

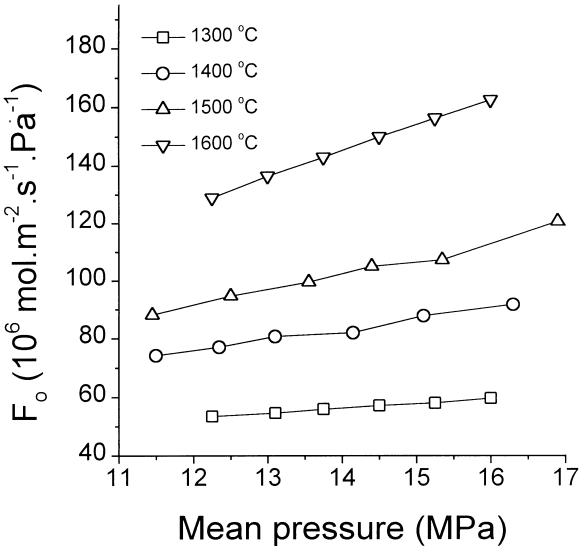

Fig. 10. Plots of permeability in the mullite ceramics versus mean pressure.

Table 1
The diffusion constants of the gelcasts fired at different temperatures

	Temperature (°C)			
	1300	1400	1500	1600
C_1	33.4	32.8	23.4	20.9
C_2	1.63	3.59	5.64	8.85

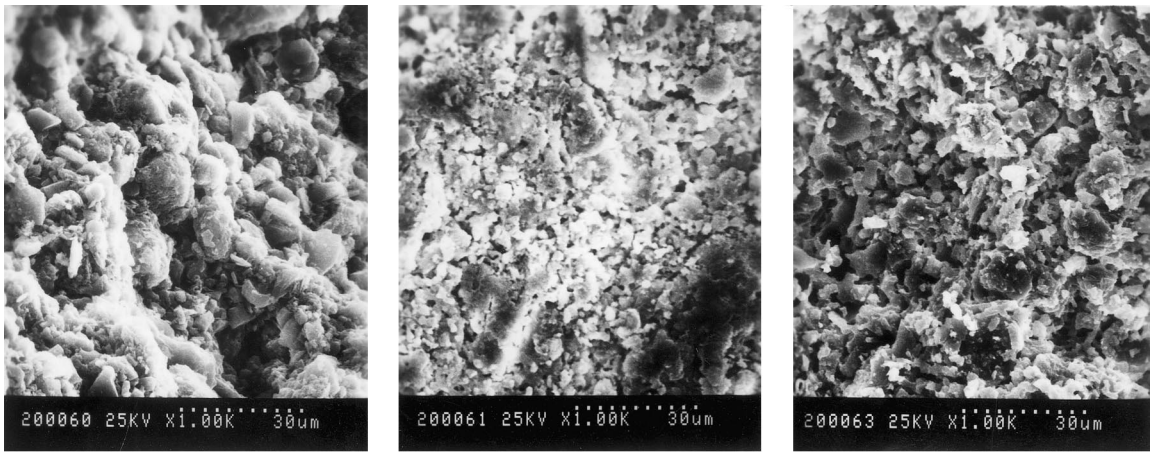

Fig. 11. Scanning electron microscopy photographs of the fracture surfaces of gelcasted mullite ceramics: (a) green body; (b) fired at 1500°C/5 h; (c) fired at 1600°C/5 h.

between F_o and P_m for the specimens fired at different temperatures. The values of C_1 and C_2 for each temperature can be obtained by fitting the plots into straight lines, and the results are listed in Table 1. As the firing temperature rises, C_1 decrease continuously while C_2 changes in reverse from 1400 to 1600°C. It suggests that laminar flow take more effect than Knudsen diffusion as the specimens were fired at higher temperatures.

As we see from Fig. 7, the mean pore size for the specimen fired at 1300°C is around 0.67 μm, which is rather smaller than that fired at 1600°C (1.31 μm). Moreover, the pore size distribution for 1600°C is much broader than low temperatures, and more big pores appear for the high-temperature samples. Therefore, laminar flow is attributed to those big pores, and it dominates the gas diffusion gradually with the increasing sintering temperature.

3.5. SEM of the specimens

The SEM photographs of the fracture surfaces of gelcasted mullite ceramics (~71.8 wt.% Al_2O_3) are shown in Fig. 11. Fig. 11a displays the morphology of green body, which consists of granulated or flaky kaolinite, granulated aluminum hydroxide, and flocculent polymer. Fig. 11b indicates that uniformed small pores formed after firing the specimen at 1500°C for 5 h. When firing at higher temperature such as 1600°C for 5 h (Fig. 11c); however, the pore sizes of the specimen grow remarkably. In addition, the glassy substance diminishes and the particle size is also bigger for the specimen fired at 1600°C than that of 1500°C. Thus, the bigger mean pore sizes in Fig. 7 at higher temperature are related to both of the glassy-phase-lessening and particle-size-augmentation.

4. Conclusions

1. The gelcasting process has been successfully employed to fabricate porous mullite ceramics.
2. The properties of porous ceramics such as porosity, average pore size, pore size distribution and gas flux can be controlled by adjusting the preparation conditions (e.g. raw material ratio and sintering temperature). The open porosity, average pore size and nitrogen flux of the mullite ceramics (~71.8 wt.% Al_2O_3) sintered at 1300–1600°C are around 58.5–63.9%, 0.76–1.31 μm, and 526–1240 $m^3\ m^{-2}\ bar^{-1}\ h^{-1}$, respectively. The mean pore sizes are related to both of the glassy-phase-lessening and particle-size-augmentation.
3. The gas permeability of the specimens is more dependent on the average pore size than the open porosity. The gas transportation in porous mullite ceramics is affected by both of Knudsen diffusion and laminar flow, and it is dominated by the later when the specimens are fired at high temperatures.

Acknowledgements

The authors thank the Chinese National Natural Science Foundation and Anhui Province Natural Science Foundation for their financial support.

References

[1] N.O. Engin, A.C. Tas, Manufacture of macroporous calcium hydroxyapatite bioceramics, J. Eur. Ceram. Soc. 19 (13–14) (1999) 2569–2572.
[2] Z.R. Ismagilov, R.A. Shkrabina, N.A. Koryabkina et al., Porous

alumina as a support for catalysts and membranes. Preparation and study, React. Kinet. Catal. Lett. 60 (2) (1997) 225–231.
[3] Y.M. Jo, Characterization of ceramic composite membrane filters for hot gas cleaning, Powder Technol. 91 (1) (1997) 55–62.
[4] M. Bennasar, D. Rouleau, R. Mayer et al., Ultrafiltration of milk on mineral membranes: improve performance, J. Soc. Dairy Technol. 35 (2) (1982) 43–49.
[5] A.J. Burgraaf, L. Cot, in: Fundamentals of Inorganic Membrane Science and Technology, Membrane Science and Technology Series 4, A.J. Burgraaf and L. Cot (Eds.), Elsevier Science BV, Amsterdam, 1996.
[6] J. Coronas, M. Menendez, J. Santamaria, Methane oxidative coupling using porous ceramic membrane reactors, Chem. Eng. Sci. 49 (12) (1994) 2005–2013.
[7] R.A. Terpstra, B.C. Bonekamp, H.J. Veringa, Preparation, characterization and some properties of tubular alpha alumina ceramic membranes for microfiltration and as a support for ultrafiltration and gas separation membranes, Desalination 70 (1988) 395–404.
[8] H. Katsuki, S. Furuta, A. Shiraishi et al., Porous mullite honeycomb by hydrothermal treatment of fired kaolin bodies in NaOH, J. Porous Mater. 2 (4) (1996) 299–305.
[9] Y. Saito et al., Effect of calcining conditions of kaolinite on pore structures of mesoporous materials prepared by the selective leaching of calcined kaolinite, J. Porous Mater. 3 (4) (1996) 233–239.
[10] H. Katsuki et al., Conventional versus microwave-hydrothermal leaching of glass from sintered kaolinite to make porous mullite, J. Porous Mater. 3 (2) (1996) 127–131.
[11] H. Katsuki, H. Takagi, O. Matsuda, Fabrication and properties of mullite ceramics with needle-like crystals, Ceram. Trans. 31 (1993) 137–146.
[12] T. Kenkyu, Preparation of mullite ceramics from allophane, Kenyu Hokoku-Tochigi-Ken Ken'nan Kogyo Shidosho 6 (1992) 24–30.
[13] A.C. Young, O.O. Omatete, M.A. Janney et al., Gelcasting of alumina, J. Am. Ceram. Soc. 74 (3) (1991) 612–618.
[14] D.M. Baskin, M.H. Zimmerman, K.T. Faber, Forming single-phase laminates via the gelcasting technique, J. Am. Ceram. Soc. 80 (11) (1991) 2929–2932.
[15] Y.F. Gu, X.Q. Liu, G.Y. Meng et al., Porous YSZ ceramics by water-based gelcasting, Ceram. Int. 25 (8) (1999) 705–709.
[16] H.T. Wang, S. Xie, W. Lai et al., Preparation and characterization of perovskite ceramic powders by gelcasting, J. Mater. Sci. 34 (6) (1999) 1163–1167.
[17] J. Sun, I. Gao, J.K. Guo, Gelcasting of nano-sized Y-TZP, J. Inorg. Mater. 13 (1998) 733–738.
[18] G. Geiger, Gelcasting automation, Am. Ceram. Soc. Bull 78 (5) (1999) 20.
[19] G.M. Brindley, M. Nakahira, Kaolinite–mullite reaction series: I–III, J. Am. Ceram. Soc. 42 (7) (1959) 311–314.
[20] R.J.R. Uhlhorn, M.H.B.J. Huis In't Veld, K. Keizer et al., Synthesis of ceramic membranes, J. Mater. Sci. 27 (1992) 527–537.